Journal of Materials Chemistry C

Accepted Manuscript

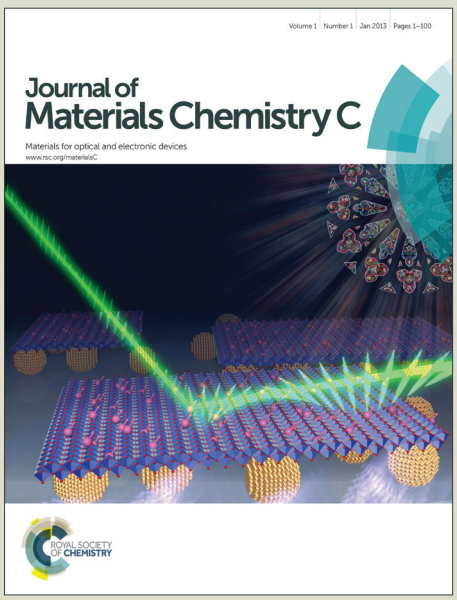

ROYAL SOCIETY OF CHEMISTRY

www.rsc.org/materialsC

Journal Name

RSCPublishing

ARTICLE

Electrochromic Properties of Self–Organized Multifunctional V_2O_5–Polymer Hybrid Films

Cite this: DOI: 10.1039/x0xx00000x

U. Tritschler[a], F. Beck[a], H. Schlaad*[b,c] and H. Cölfen*[a]

Received ooth January 2012,
Accepted ooth January 2012

DOI: 10.1039/x0xx00000x

www.rsc.org/

Bio-inspired V_2O_5–polymer hybrid films were prepared following a one-step self-organization procedure based on liquid crystal (LC) formation of organic and inorganic components. These materials were previously reported to exhibit advantageous mechanical properties, comparable to biomaterials, such as human bone and dentin. Here, we show that these hybrid films prepared via a fast and simple synthesis procedure have an additional function as an electrochromic material, exhibiting a long-term cycle stability under alternating potentials. The structures were found to remain intact without visible changes after more than hundred switching cycles and storing the devices for several weeks. Consequently, this multifunctional V_2O_5–polymer hybrid system shows great promise for various technical applications.

Organic-inorganic biomaterials, such as bone and nacre, consist of high, stiff and brittle, mineral fractions, which are embedded in a soft organic matrix.[1, 2] These materials exhibit a pronounced hierarchical structure and a controlled coupling at the interface between organic and inorganic components. These structural characteristics contribute to their outstanding mechanical properties, combining both high stiffness and toughness.[3-6] Very recently, we developed a biomimetic fabrication concept for the synthesis of organic-inorganic composites based on liquid crystal (LC) formation of organic and inorganic components.[7] The LC 'gluing' polymer used was a statistical polyoxazoline with pendant cholesteryl and carboxy side chains, enabling the polymer, on the one hand, to form chiral-nematic lyotropic phases on the length scale of several hundreds of micrometers upon shearing, and on the other hand, to selectively bind to nanoparticle faces via electrostatic interactions or hydrogen brides.[7, 8] The inorganic nanoparticles, Laponite[7] and vanadium pentoxide (V_2O_5),[8] are anisotropic in shape and consequently, were also able to form LC phases. V_2O_5–LC polymer composites structured on six hierarchical levels exhibiting a well-defined nanostructure and a hierarchical structuring on the length scale of several hundreds of micrometers were fabricated via this one-step self-organization process.[8] Long-range orientation of the polymeric lyotropic phase was induced by rotational shearing by means of a shear cell. Remarkably, these materials exhibit advantageous mechanical properties, comparable to mechanical properties of natural hierarchically structured organic-inorganic composites like human bone and dentin (data obtained by nanoindentation).[8] In this study, we investigated these materials regarding their electrochromic performance, a second feature of this composite system, besides mechanical reinforcement.

Electrochromism of thin films of transition-metal oxides, such as tungsten oxide (WO_3) or V_2O_5, have been previously studied. Upon cation intercalation (reduction) of the metal oxide, a change in absorbance in the visible region and consequently, a change in colour of the material, is observed.[9] Different methods to produce appropriate electrochromic films were reported, such as sputtering,[10] spin-coating,[11-13] and electrodeposition.[14-16] Electrochromic devices often find application, in e.g. smart windows, due to their low operating potential and the memory effect, allowing to retain the respective oxidation state with a small amount or without any additional power.[17, 18] Recent developments of electrochromic materials leading to increased electrochromic performance in terms of e.g. higher coloration efficiencies and faster response times include the use of ordered mesoporous and interconnected inorganic structures, giving rise to a good ion excess and high electric conductivities.[14, 15, 19, 20] An issue regarding technical applications is the development of mechanically resistant electrochromic films with low susceptibility to cracking under mechanical stress. These properties are difficult to achieve with purely inorganic and mesoporous structures, which are expected to be mechanically stiff and brittle. However, promising results in achieving flexible electrochromic metal oxide films (WO_3 and V_2O_5) were recently reported.[21-24] These films were obtained by depositing the respective nanoparticle dispersion on flexible plastic substrates via an inkjet printing technique. Another mechanically attractive system with potential advantageous electrochromic properties may be our bio-inspired V_2O_5–LC polymer composite. The mechanical properties of composites were investigated by using specimens with a thickness in the range of several tens to hundreds of micrometers. Considering, that films with nanometer scale thickness are known to become even more insensitive to flaws on the nanoscale, compared to micron-sized films,[25] thin V_2O_5–LC polymer hybrid films become very attractive for potential technical applications.

V_2O_5–LC polymer hybrid particles were synthesized by adding an aqueous dispersion of LC 'gluing' copolymer (see Figure S1 in the supporting information (SI)) to an isotropic V_2O_5 dispersion and stirring the mixture overnight, allowing the polymer to bind to the particles, followed by a phase-transfer from aqueous medium to THF, as reported previously.[8] For

investigating the electrochromic behaviour of our V_2O_5–LC polymer composites, hybrid films with a thickness in the range of ca. 100-300 nm (data obtained by a profilometer, see Figure S2 in the SI) were prepared by spin-coating V_2O_5–LC polymer hybrid dispersions (~3 wt%) on an ITO coated glass substrate, inducing shearing and consequently, long-range orientation of the polymeric lyotropic phase. The electrochromic device was assembled with a second ITO coated glass slide acting as counter electrode, separated from the working electrode by means of a thermoplastic gasket as distance holder and filled with 1 M lithium bis(trifluoromethylsulfonyl) imide in propylene carbonate, before fixing the platinum wire, acting as a reference electrode, and sealing the cell with epoxy glue (see Figure S3 in the SI). The fabricated thin, yellow V_2O_5–LC polymer hybrid films were suitable for observing optical changes via UV-visible spectroscopy, exhibiting maximum absorbance values in the range of ca. 0.15 to 0.3 at a wavelength of ~450 nm (oxidized state; see transmittance spectra in Figure 1). A cathodic potential of -0.5 V led to lithium intercalation into V_2O_5, resulting in a rather homogenous bleaching (green/gray) with a transmittance of 0.77 at a wavelength of 450 nm of the prior yellow hybrid film, which exhibited a transmittance of 0.52 at 450 nm (Figure 1). Upon applying an anodic potential of 1.5 V, which induces lithium extraction, the colour of the film turned back into yellow with an increase in absorption in the 400-500 nm range, similar as reported for V_2O_5 films.[11, 14, 15, 26]

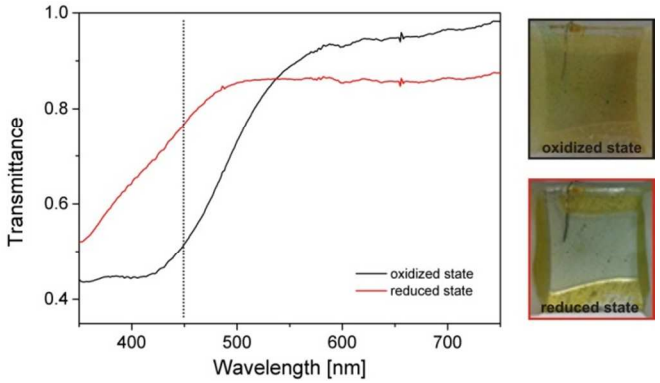

Figure 1. Optical transmittance spectra of V_2O_5–LC polymer hybrid films in the oxidized state (black) and reduced state (red) under alternating potentials of -0.5 V and 1.5 V (sweep rate of 50 mV s^{-1}), and example images of hybrid films in the oxidized and reduced state. Change in transmittance was observed at a wavelength of 450 nm (dotted line).

Cycling stability of the V_2O_5–LC polymer hybrid films was investigated under alternating potentials between -0.5 V and 1.5 V (sweep rate of 50 mV s^{-1}) by observing the transmittance at 450 nm via time-resolved UV-visible spectroscopy. After equilibration of the system achieved after few switching cycles, the composite structures showed distinct transitions between intercalated (reduced/bleached) state and deintercalated (oxidized/coloured) state with a change in transmittance of ~25% at 450 nm and a good long-term cycle stability with a decrease of less than ~20% over more than hundred switching cycles (Figure 2 and Table 1). Similar stabilities of V_2O_5 and WO_3 mesoporous structures were reported by Steiner et al.[14, 15, 20] and Brezesinski and Smarsly et al.,[27] respectively.

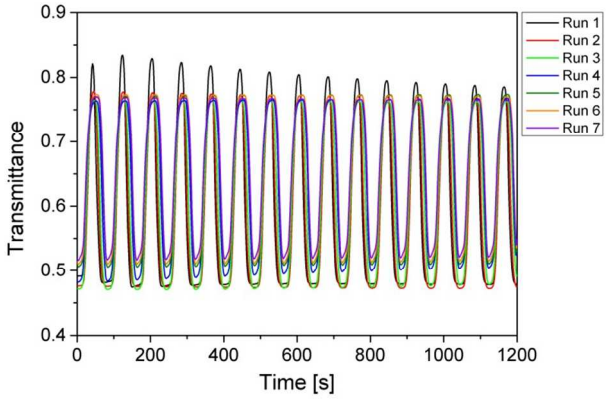

Figure 2. Cycling stability of V_2O_5–LC polymer hybrid films was investigated by applying alternating potentials (-0.5 V – 1.5 V; sweep rate of 50 mV s^{-1}). The transmittance change was recorded at a wavelength of 450 nm. After equilibration, the decrease in transmittance over 100 cycles was less than 20%. Selected transmittance values and switching times are shown in Table 1.

Table 1. Overview of transmittance change, switching times for bleaching (reduction) and coloration (oxidation), charge per area (Q) and coloration efficiency (CE) values for ion insertion (reduction) and extraction (oxidation) for a V_2O_5–LC polymer hybrid film observed at a wavelength of 450 nm during voltammetric cycling between -0.5 V and 1.5 V (sweep rate of 50 mV s^{-1}). The switching behavior of the film position before storing the device is graphically illustrated in Figure 2.

Cycle	ΔT [%]	τ_b [s]	τ_c [s]	Q [mC cm^{-2}]		CE[a] [cm^2 C^{-1}]	
				insert.	extract.	insert.	extract.
1	33	20	23	3.9	3.7	-86	-89
20[b]	30	22	24	3.9	3.8	-77	-80
100	25	27	20	3.4	3.0	-72	-83
after storing	20	27	24	3.5	3.1	-56	-64

[a]CE is defined as the difference of the optical density between oxidized and reduced state at 450 nm divided by the inserted/extracted charge per area.[28] Note that CEs may vary within the hybrid film due to height variations of the films (see profile plot in Figure S2) and consequently, varying optical densities. [b]After equilibration of the system.

Even after performing a hundred switching cycles and storing the electrochromic devices in the oxidized i.e. yellow state for over 1 month without cycling, the structures exhibited good cycle stability showing only negligible decreases in the transmittance change relative to the transmittance change obtained after a hundred switching cycles before storing the cell. Due to height variations within the hybrid film (see profile plot, Figure S2) and thus, locally slightly dependent initial transmittance values, the change in transmittance of the switching curves before and after storing varied to some extent. The switching curve obtained after storing the device (see Figure S4) exhibits a slightly lower initial absorbance (higher transmittance) compared to the switching curve recorded before storing. Consequently, the change in transmittance between oxidized and reduced state and thus, the coloration efficiencies were lower after storing (<20%, see Table 1 and Figure S4). When using film positions with very similar initial transmittance values, the decrease in transmittance change after storing the cell was found to be only ~8% lower than the transmittance change observed after over 100 redox cycles before storing the device (see Figure S5 in the SI), suggesting that storing the device for several weeks did not significantly influence the cycling behaviour of the hybrid films.

As for example already observed by Wang et al.,[11] the contrast ratio of the V_2O_5–LC polymer hybrid films can be adjusted by varying the film thickness, i.e. the transmittance change between oxidized and reduced state increases with increasing film thickness (transmittance change of 12% for a hybrid film with a transmittance of ~0.7 at 450 nm in the oxidized state (Figure S5) compared to 25% for a hybrid film with a minimum transmittance of ~0.5 at 450 nm).

Stability of the V_2O_5–LC polymer hybrid films towards constant positive or negative voltages was investigated by applying positive or negative potentials for a time period of ca. 5 min, followed by cycling between -0.5 V and 1.5 V (sweep rate of 50 mV s^{-1}). Applying a constant positive voltage of 1.5 V and 2 V over ca. 5 min, respectively, did not lead to a change in transmittance difference, revealing that the films are stable under these conditions. In case the film was kept in the reduced state for ~5 min (-0.5 V, -0.7 V or -1 V), a drastic decrease to ca. 8% of the original transmittance change was observed, probably due to irreversible structural changes occurring upon applying longer negative potentials, leading to a decrease in reversible lithium insertion sites.[11]

An example cyclic voltammogram obtained from the V_2O_5–LC polymer hybrid thin film shown in Figure 1 and Figure 2 is illustrated in Figure S6, exhibiting two peaks at 0.12 V and -0.32 V for lithium insertion (reduction step) and two peaks at 0.22 V and 0.78 V for lithium extraction (oxidation step), similar as reported for thin vanadium oxide films, prepared e.g. by spin-coating.[11] The amount of inserted and extracted charge during repetitive cycling between -0.5 V and 1.5 V did not differ significantly. ~90% of the inserted charge during a reduction step was extracted in the subsequent oxidation step, leading to a high cycling reversibility (Figure 3) and consequently, confirming data obtained by UV-visible spectroscopy (Figure 2).

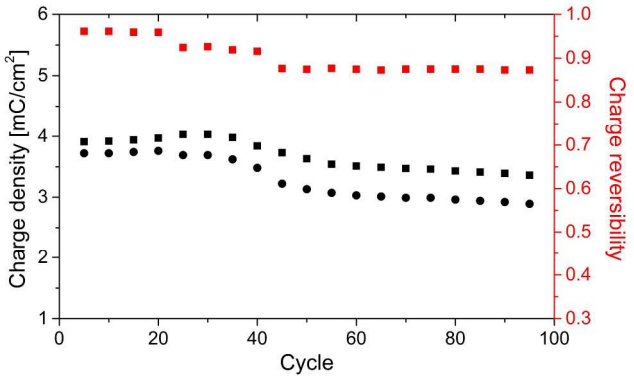

Figure 3. Charge density of reduction steps (black squares) and oxidation steps (black circles) and corresponding charge reversibility (red) of V_2O_5–LC polymer hybrid films obtained during repetitive voltammetric cycling between -0.5 V and 1.5 V with a sweep rate of 50 mV s^{-1}. Data of every fifth switching cycle out of 100 cycles are illustrated.

Coloration efficiencies[28] of the film position of which the transmittance data at a wavelength of 450 nm are illustrated in Figure 2 are comparably high with ca. -77 cm^2 C^{-1} (for reduction, see Table 1) and -80 cm^2 C^{-1} (for oxidation, see Table 1) compared to coloration efficiencies of reported thin V_2O_5 films which were, for example, prepared by spin-coating (ca. -20 cm^2 C^{-1} at a wavelength of 850 nm)[11] and inkjet printing (up to -42 cm^2 C^{-1} at 750 nm).[24] In contrast, the highest coloration efficiencies for V_2O_5 up to date with ca. -3400 cm^2 C^{-1} (for reduction; at 430 nm) and -3600 cm^2 C^{-1} (for oxidation; at 430 nm) were obtained from micrometer-thick mesoporous V_2O_5 films exhibiting a transmittance change of ~50% and a cycle stability up to ca. 100 cycles with a decrease of <20% in coloration contrast.[14]

The relatively symmetric bleaching and coloration steps indicate similar response times of the V_2O_5–LC polymer hybrid films for reduction and oxidation. The response times of Δt_{ox} ~ 20-24 s and Δt_{red} ~ 20-27 s, for colored (oxidized) and bleached (reduced) state, respectively, were determined by measuring the time period between an absorbance of 90% and the maximum/minimum of absorbance (see Table 1 and Figure S7). Response times obtained via this method correlate with the timescale observed by human eye, compared to response times calculated based on Gaussian or Boltzmann distributions.[27] The relative slow response times may be attributed to the slow diffusion of lithium ions through the hybrid material,[14, 29] most likely due to the presence of the compliant organic phase. In order to increase the Li^+ diffusion rate within the densely-packed V_2O_5-polymer hybrid particle layers, [8] a highly conductive room temperature ionic liquid triethylsulfonium bis(trifluoromethylsulfonyl) imide was added during film formation (30-60 wt% with respect to hybrid particles). However, the ionic liquid did not significantly influence the switching speed. Similar coloration and bleaching times were reported by Brezesinski and Smarsly et al.[27] for non-porous crystalline WO_3 thin films, whereas response times of the corresponding mesoporous counterparts were significantly reduced. The response times of the V_2O_5–LC polymer hybrid films are shorter compared to the response times reported for flexible V_2O_5 films prepared by inkjet printing (up to 100 s; taken from absorption spectra).[24] Recently, Steiner et al.[14, 15] reported about micrometer-thick mesoporous V_2O_5 films exhibiting remarkable fast response times in the range of seconds to milliseconds. Disadvantage of these completely inorganic and mesoporous template structures, however, is expected to be their significantly lower mechanical strength compared to our organic-inorganic composite system. Additionally, when damaged under mechanical stress, these porous structures may lose their advantageous electrochromic performance. A second drawback of such mesoporous V_2O_5[14] structure compared to our V_2O_5–LC polymer hybrid system is the more complex, multistage fabrication procedure. This includes the synthesis of a mesoporous polymer network, followed by electrodeposition of vanadium pentoxide in the voids and subsequent dissolution of the polymer matrix.

Structural investigations on the hybrid films were performed before and after about hundred redox cycles by polarized optical light microscopy (Abrio) and scanning electron microscopy (SEM). Abrio imaging allows to study quantitatively structural orientations by measuring the magnitude of retardance and the azimuthal data at every image point. Different structural orientations are illustrated by different colors, re-assigned to a particular orientation by means of a color code (represented by the color wheel). Domains with the same color and consequently, the same structural orientation were observed on the length scale of up to tens of micrometers, both before and after applying alternating potentials (Figure 4a and b). First, the formation of lyotropic regions with the same orientation after spin-coating a ~3wt% dispersion of hybrid particles suggests a significant influence of the LC polymer on the alignment of V_2O_5 ribbons. Note that the hybrid synthesis was initiated by using an isotropic V_2O_5 dispersion. And second, the size of the domains with same

structural orientation did not change before and after cycling, indicating that alternating potentials did not significantly affect the structural orientation on the micron scale.

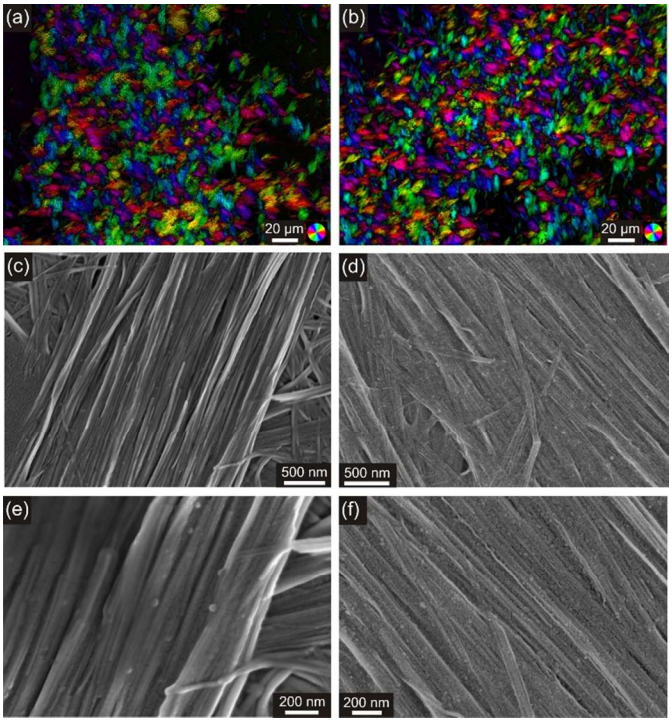

Figure 4. Quantitative birefringence optical micrographs (a,b) and SEM images (c-f) of V_2O_5–LC polymer hybrid films before and after voltammetric cycling (left and right columns, respectively).

SEM analysis confirms the observed structural orientation before and after voltammetric cycling of the films on the lower micrometer length scale (Figure 4c and d). SEM images also revealed that hybrid particles are not completely homogenously distributed throughout the composite film (data not shown), thus confirming the observed height differences on the nanometer scale in contour plots (see Figure S2 in the SI). The vanadia structures look similar before and after potential cycling, although the fiber surface tends to be rougher after cycling, with small cracks appearing throughout the hybrid film, probably due to lithium intercalation and extraction processes (Figure 4e and f). Obviously, applying alternating potentials did not change the structure of the hybrid films on the micro- to nanometer length scale.

In summary, a multifunctional V_2O_5–LC polymer hybrid system was developed via a one-step self-organization. In a previous study, we reported about the structuring of this composite system on six hierarchical levels covering the milli-, micro- and nanometer length scales.[8] These composites exhibited advantageous mechanical properties, comparable to organic-inorganic biomaterials like human bone and dentin.[8] Here, we highlighted a second feature of this hybrid system. The vanadia-polymer structures exhibit good electrochromic performance with long-term cycle stability. The defined structuration remained intact during extended voltammetric cycling. Potential cycling was performed under normal conditions, revealing resistance of the electrochromic device towards moisture and oxygen. Due to the increased mechanical strength of the hybrid films compared to purely inorganic and mesoporous electrochromic templates and the simple, fast and cost-efficient preparation method of the V_2O_5–LC polymer hybrid films, this bio-inspired system possesses a couple of important characteristics in terms of technical applications, making it a potential candidate for smart and flexible electrochromic windows. In order to consider this hybrid system for technical applications, we currently investigate the stability of the hybrid films over more extended periods of time (up to one year) and aim at improving the device construction for flexible electrochromic films. For example, the transparent conductive coating used here is ITO, which is brittle and a relatively expensive material, which needs to be replaced by a flexible transparent electrode, for instance by a silver electrode as reported by Layani et al.[21]

Acknowledgements

The authors thank Rainer Winter, Michael Linseis and Stefan Scheerer as well as Maik Scherer for fruitful discussions. Financial support by DFG priority program 1420 is gratefully acknowledged.

Notes and references

[a] University of Konstanz, Physical Chemistry, Universitätsstraße 10, D-78457 Konstanz, Germany. E-mail: helmut.coelfen@uni-konstanz.de
[b] Max Planck Institute of Colloids and Interfaces, Department of Colloid Chemistry, Research Campus Golm, D-14424 Potsdam, Germany.
[c] University of Potsdam, Institute of Chemistry, Karl-Liebknecht-Straße 24-25, D-14476 Potsdam, Germany. E-mail: schlaad@uni-potsdam.de

† Electronic Supplementary Information (ESI) available: Experimental details and additional figures. See DOI: 10.1039/b000000x/

1. F. C. Meldrum and H. Cölfen, *Chem. Rev.*, 2008, **108**, 4332-4432.
2. H. A. Lowenstam and S. Weiner, *On Biomineralization*, Oxford University Press, New York, 1989.
3. B. Aichmayer and P. Fratzl, *Phys. J.*, 2010, **9**, 33-38.
4. P. Fratzl and R. Weinkamer, *Prog. Mater. Sci.*, 2007, **52**, 1263-1334.
5. R. O. Ritchie, *Nat. Mater.*, 2011, **10**, 817-822.
6. I. Jäger and P. Fratzl, *Biophys. J.*, 2000, **79**, 1737-1746.
7. U. Tritschler, I. Zlotnikov, P. Zaslansky, B. Aichmayer, P. Fratzl, H. Schlaad and H. Cölfen, *Langmuir*, 2013, **29**, 11093-11101.
8. U. Tritschler, I. Zlotnikov, P. Zaslansky, P. Fratzl, H. Schlaad and H. Cölfen, *ACS Nano*, 2014, **8**, 5089-5104.
9. A. A. Argun, P.-H. Aubert, B. C. Thompson, I. Schwendeman, C. L. Gaupp, J. Hwang, N. J. Pinto, D. B. Tanner, A. G. MacDiarmid and J. R. Reynolds, *Chem. Mater.*, 2004, **16**, 4401-4412.
10. A. Talledo and C. G. Granqvist, *J. Appl. Phys.*, 1995, **77**, 4655.
11. Z. Wang, J. Chen and X. Hu, *Thin Solid Films*, 2000, **375**, 238-241.
12. Y. Shimizu, K. Nagase, N. Miura and N. Yamazoe, *Solid State Ionics*, 1992, **53–56, Part 1**, 490-495.
13. K. Nagase and Y. Shimizu, *Appl. Phys. Lett.*, 1992, **60**, 802.
14. M. R. J. Scherer, L. Li, P. M. S. Cunha, O. A. Scherman and U. Steiner, *Adv. Mater.*, 2012, **24**, 1217-1221.
15. L. Li, U. Steiner and S. Mahajan, *J. Mater. Chem.*, 2010, **20**, 7131-7134.
16. P. Liu, S.-H. Lee, C. E. Tracy, J. A. Turner, J. R. Pitts and S. K. Deb, *Solid State Ionics*, 2003, **165**, 223-228.
17. D. R. Rosseinsky and R. J. Mortimer, *Adv. Mater.*, 2001, **13**, 783-793.
18. G. A. Niklasson and C. G. Granqvist, *J. Mater. Chem.*, 2007, **17**, 127-156.
19. A. Walcarius, *Chem. Soc. Rev.*, 2013, **42**, 4098-4140.
20. D. Wei, M. R. J. Scherer, C. Bower, P. Andrew, T. Ryhänen and U. Steiner, *Nano Lett.*, 2012, **12**, 1857-1862.

21. M. Layani, P. Darmawan, W. L. Foo, L. Liu, A. Kamyshny, D. Mandler, S. Magdassi and P. S. Lee, *Nanoscale*, 2014, **6**, 4572-4576.
22. P. J. Wojcik, A. S. Cruz, L. Santos, L. Pereira, R. Martins and E. Fortunato, *J. Mater. Chem.*, 2012, **22**, 13268-13278.
23. C. Costa, C. Pinheiro, I. Henriques and C. A. T. Laia, *ACS Appl. Mater. Interfaces*, 2012, **4**, 1330-1340.
24. C. Costa, C. Pinheiro, I. Henriques and C. A. T. Laia, *ACS Appl. Mater. Interfaces*, 2012, **4**, 5266-5275.
25. H. Gao, B. Ji, I. L. Jäger, E. Arzt and P. Fratzl, *Proc. Natl. Acad. Sci. U.S.A.*, 2003, **100**, 5597-5600.
26. Y. Wang and G. Cao, *Electrochim. Acta*, 2006, **51**, 4865-4872.
27. T. Brezesinski, D. Fattakhova Rohlfing, S. Sallard, M. Antonietti and B. M. Smarsly, *Small*, 2006, **2**, 1203-1211.
28. P. M. S. Monk, R. J. Mortimer and D. R. Rosseinsky, *Electrochromism and Electrochromic Devices*, Cambridge University Press, Cambridge, 2007.
29. S. I. Cho, W. J. Kwon, S. J. Choi, P. Kim, S. A. Park, J. Kim, S. J. Son, R. Xiao, S. H. Kim and S. B. Lee, *Adv. Mater.*, 2005, **17**, 171-175.